Tribology International 199 (2024) 110007

Contents lists available at ScienceDirect

Tribology International

journal homepage: www.elsevier.com/locate/triboint

Tribological performance of green nanolubricants using functionalized $CaCO_3$ nanoparticles

José M. Liñeira del Río [a,b,*], Carlos M.C.G. Fernandes [b,c], David E.P. Gonçalves [b], Jorge H. O. Seabra [c]

[a] Laboratory of Thermophysical and Tribological Properties, Nafomat Group, Department of Applied Physics, Faculty of Physics and Institute of Materials (iMATUS), Universidade de Santiago de Compostela, Santiago de Compostela 15782, Spain

[b] INEGI, Universidade do Porto, Campus FEUP, Rua Dr. Roberto Frias 400, Porto 4200–465, Portugal

[c] Faculdade de Engenharia, Universidade do Porto, Rua Dr. Roberto Frias s/n, Porto 4200–465, Portugal

ARTICLE INFO

Keywords:
Biolubricants
Nanoparticles
Functionalization
Surface analysis

ABSTRACT

In response to the mounting concern over environmental pollution and the depletion of petroleum reserves, biolubricants have emerged as a promising alternative to mineral oil-based lubricants. Thus, the aim of this research is the tribological characterization of green castor and soybean nanolubricants containing functionalized $CaCO_3$ nanoparticles. Friction improvements were reached with maximum friction decreases of 14 % and 18 % compared to castor and soybean oils. Concerning wear, optimal concentration for castor and soybean nanolubricants was intermediate concentration of 0.15 wt% with width wear reductions of 27 % and 24 % compared to castor and soybean oils, respectively. Tribological mechanisms of tribofilm formation, repairing and rolling-bearing were identified. In rolling-sliding tests, the use of nanoparticles was crucial at low speeds with outstanding friction reductions.

1. Introduction

Nowadays, the conservation of materials and energy is a crucial issue, being the major reason of energy loss in mechanical systems the friction and produced wear that could be decreased by means of lubrication. Thus, around 90 % of the internal elements of earthmoving machinery are lubricated [1], being more than 95 % of the used lubricants from a mineral nature [2], but these type of petroleum-based lubricants have numerous issues and dangerous impacts on the environment. Hence, mineral lubricants are made from crude oil through typical oil refining processes and comprise several chemical components, therefore having an elevated ecotoxicity and a poor biodegradability [3]. It is calculated that 20 % of around 5 million tons of lubricant used every year in Europe is released to environment. One kilogram of a mineral oil is able to pollute a million liters of water [4]. Consequently, contamination produced by lubricants is far from irrelevant. Additionally, mineral lubricants can also contaminate the soil and the air owing to their volatility [5]. Some investigations have documented the adverse effects of mineral lubricants on human health, since chronic inhalation or dermal exposure to these lubricants can consequence in inflammatory effects on the respiratory system and the site of contact, while also being carcinogenic [6]. In this perspective, environmentally improved lubricants have become more important in industrial applications, therefore biolubricants are promising as a substitute to the aforementioned mineral lubricants to evade their damaging effects [7], because biolubricants are degradable, environment-friendly, clean, and therefore pose little or no risk to the environment or operators [8]. Furthermore, Miller et al. [9] perform a comparative life cycle analysis between petroleum and soybean lubricants considering carbon sequestration and end-of-life impacts. This analysis determined that soybean oil lubricants had a significantly reduced impact on climate change and fossil fuel use. With biodegradable and nontoxic nature, vegetable oils obtain their appropriate place as a base oil for biolubricants. The enhancement of biodegradable lubricants is very valuable for the environment as they decompose 100 % and does not damage the environment. Applying biolubricants in industrial applications would help decrease friction and wear. Apart from the major advantages, there are many issues that must be resolved

* Corresponding author at: Laboratory of Thermophysical and Tribological Properties, Nafomat Group, Department of Applied Physics, Faculty of Physics and Institute of Materials (iMATUS), Universidade de Santiago de Compostela, Santiago de Compostela 15782, Spain.

E-mail address: josemanuel.lineira@usc.es (J.M. Liñeira del Río).

https://doi.org/10.1016/j.triboint.2024.110007
Received 2 July 2024; Received in revised form 16 July 2024; Accepted 17 July 2024
Available online 18 July 2024

Table 1
Main tribological findings found with biolubricants using NPs as additives.

Lubricant	NPs	Friction reduction %	Wear reduction %	Reference
Castor Oil	MoS_2	NA	NA	[21]
Sunflower Oil	CuO, ZrO_2	35, 28	11, 24	[22]
Soybean Oil	CuO, ZrO2	40, NI	5, 7	[22]
Jojoba oil	$CaCO_3$	34	40	[23]
Castor Oil	f-CuO	34	28	[24]
Rapeseed Oil	CuO, CeO_2	40, 54	NI, 10	[25]
Neem Oil	SiO_2	15	10	[26]
Palm Oil	TiO_2, CuO	8, 13	62, 40	[27]
Olive Oil	Cu, h-BN	NA	8, 17	[28]
Bio-PAO	Cu/Ti/Mn-GO	40	46	[29]

*NI= not improved, NA= not available

before effective use. These lubricants have a very restricted working temperature range, poor oxidation stability or lack of viscosity range. Therefore, to solve these issues, nanoparticles (NPs) are being included in biolubricants to reach enhancement of specific properties. A number of recent articles have demonstrated that the incorporation of NPs into lubricants can significantly reduce both friction and wear [10–13]. The principal advantages of using NPs as additives in comparison to other materials are due to their superior capabilities to reduce friction and wear, and even to repair the worn surface. This is due to the small size of NPs, which allows them to enter the contact area, resulting in a positive lubrication effect [8]. Moreover, due to these unique properties NPs can also be used in other systems, for example as reinforcement in different alloy matrix finding interesting results [14,15]. Furthermore, several researchers have verified that adding some NPs to biodegradable lubricant oils, better improvement of tribological performance was reached [16–20]. Thus, Table 1 summarizes the main tribological findings using biodegradable nanolubricants.

For example, Yu et al. [21] examined the tribological performance of MoS_2 NPs in castor oil. They observed that MoS_2 NPs reduced the friction and adhesive wear. Furthermore, Kumar and Gautam [22] investigated the tribological properties of vegetable oil-based nanolubricants composed by soybean and sunflower oils with CuO and ZrO_2 NPs. These authors found that using CuO NPs as additives of both vegetable oils improved antifriction behavior with reductions in friction around 40 %. Regarding the ZrO_2 NPs, the addition to sunflower oil led to a 28 % reduction in friction and 24 % in wear. Additionally, Mousavi et al. [29] studied the tribological performance of a novel synthetic biodegradable PAO using Cu/TiO_2/MnO_2-doped GO nanocomposites as additives, achieving significant friction and wear enhancements.

Despite these encouraging results, one of the greatest challenges in the formulation of nanolubricants is their poor stability due to the sedimentation of NPs [30,31]. The stability of nanofluids can be achieved through two distinct stabilization mechanisms: electrostatic stabilization and steric stabilization. The first mechanism is that the aggregation of nanoparticles is inhibited due to the presence of a double layer of electric charges that envelopes the nanoparticles. In order to prevent the aggregation of nanoparticles, the repulsive forces between particles must be stronger than the attractive forces (van der Waals) [32]. On the other hand, steric stabilization entails the coating of nanoparticles with distinct molecules through surfactants or chemical modifications, thereby establishing a distance between nanoparticles that prevents their aggregation with other nanoparticles [33]. In a comprehensive review of the temporal stability of various nanolubricants, Chen et al. [31] addressed this topic. The study examined several characteristics of nanoparticles, including their size and surface modification agent. The findings indicated that surface modification is a crucial factor in the efficient dispersion of nanopowders in lubricant oils. Therefore, it is important to use surface modified nanoparticles in order to achieve good stability and a future potential use in industry for the

Table 2
Main physical properties of castor and soybean base oils.

	Viscosity (313.15 K)	Density (313.15 K)	Viscosity Index (VI) (313.15 to 373.15 K)
	η / mPa·s	ρ / g cm−3	-
Castor oil	236.6	0.9462	92
Soybean oil	28.5	0.9075	232

*Viscosity and density determined by ASTM D7042 and VI by ASTM D2270.

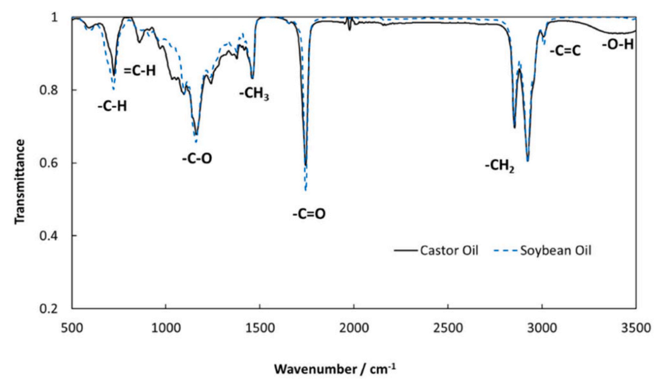

Fig. 1. FTIR spectrum of Castor oil and Soybean oil.

nanolubricant. Furthermore, the full tribological characterization (pure sliding and rolling-sliding contacts) of biolubricants is very scarce in literature. Thus, in this work, the full tribological characterization of biodegradable nanolubricants composed by two different vegetable oils: castor and soybean oils and functionalized $CaCO_3$ nanoparticles were carried out. The greatest novelty of this work is that both NPs and oils are ecofriendly, and it is difficult to find tribological works in literature with this type of lubricant system, especially, that use functionalized type NPs. $CaCO_3$ NPs are environmentally friendly and verify the European Ecolabel standards for using as lubricant additives [34]. These NPs are also eco-friendly since the surface modification agent is a fatty acid and $CaCO_3$ is one of most rich biominerals in the Earth crust, formed in geological sources like limestone. Furthermore, the experimental works of $CaCO_3$ NPs as lubricant oil additives is limited [23,35, 36]. Thus, Zhang et al. [36] analyzed the antiwear properties of $CaCO_3$ NPs as additive to PAO10 oil, viewing that $CaCO_3$ NPs can significantly improve the anti-wear properties of PAO10 base oil (around 90 % decrease in wear). Furthermore, Kulkarni et al. [23] examined the addition of $CaCO_3$ NPs in jojoba oil, reaching that non-functionalized $CaCO_3$ NPs addition to oil reveals notable antifriction and anti-wear performance, with maximum decreases around 34 % and 40 %, respectively. In comparison with our research, these authors have not studied the friction performance in rolling-sliding conditions. Additionally, in the present research two biodegradable base oils (castor and soybean) were used to obtain a greater knowledge about biodegradable lubricants.

2. Materials and procedures

2.1. Vegetable base oils

The vegetable base oils used in this research, castor oil and soybean oil, were provided by Merck (Darmstadt, Germany). The main physical properties of base oils are summarized in Table 2. Thus, Castor oil has a viscosity index of 92, a dynamic viscosity of 236.6 mPa s and a density of 0.9462 g·cm^{-3} at 313.15 K while soybean oil has a viscosity index of 232, a dynamic viscosity of 28.5 mPa s and a density of 0.9075 g·cm^{-3} at 313.15 K.

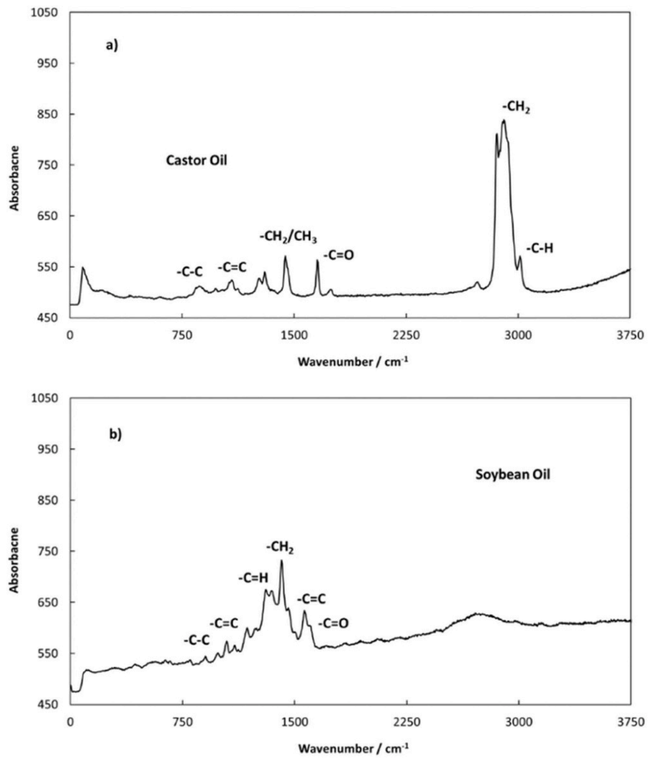

Fig. 2. Raman spectrum for Castor (a) and Soybean oils (b).

Both vegetable oils were characterized by infrared spectroscopy, FTIR, (VARIAN 670-IR spectrometer form Agilent, California, USA) and Raman spectroscopy (alpha300R+ from WITec GmBH, Kroppach, Germany) to find the main functional groups. Thus, Fig. 1 reveals the FTIR spectrum of castor oil and soybean oil. As it can be observed, for both oils the spectrum is very similar. Hence, adsorption bands around 3500 cm^{-1} are assigned to O-H stretching vibration. A small stretching vibration band at 3010 cm^{-1} is related to the C═C bond. Likewise, asymmetric and symmetric deformation vibrations of $-CH_3$ appear around 1460 cm^{-1} and 1370 cm^{-1}. Besides, two strong bands at 2930 cm^{-1} and 2840 cm^{-1} are associated to the symmetric and asymmetric stretching vibration of CH_2, respectively. Furthermore, a very strong and narrow band at 1740 cm^{-1} is linked to the C═O of ester compounds. Additionally, the bands at 1240 cm^{-1} and 1160 cm^{-1} are associated with the stretching vibration for C–O in ester group. Furthermore, a small band at 860 cm^{-1} is ascribed to the out–of–plane bending vibration of =C–H and finally the intense band at 720 cm^{-1} is characteristic of –CH for deformation vibration [37–39].

Regarding the Raman spectra of vegetable oils, as Fig. 2 shows, the spectra of castor oil and soybean oil are quite different. Fig. 2a displays de Raman spectrum of castor oil with the next characteristic peaks: The bands around 3010 cm^{-1} and 2930 cm^{-1} could be ascribed to the stretching of CH and CH_2, respectively. Furthermore, the band around 1740 cm^{-1} was ascribed to the C═O stretching of triacylglycerol structure that is present in the Castor oil. Finally, the band placed around 1440 cm^{-1} is assigned to bending of CH_2/CH_3 groups. Regarding the soybean oil Raman spectrum, Fig. 2b, the presence of the following bands are observed: 870 and 1080 cm^{-1} for C-C stretching, 970 cm^{-1} ascribed to C═C trans deformation, 1270 cm^{-1} regarding the CH= bond plane deformation; 1300 cm^{-1} related to twisting motion of methylene, 1440 cm^{-1} associated to CH_2 deformation, 1660 cm^{-1} to C═C cis stretching and finally at 1750 cm^{-1} owing to C═O stretching [40,41].

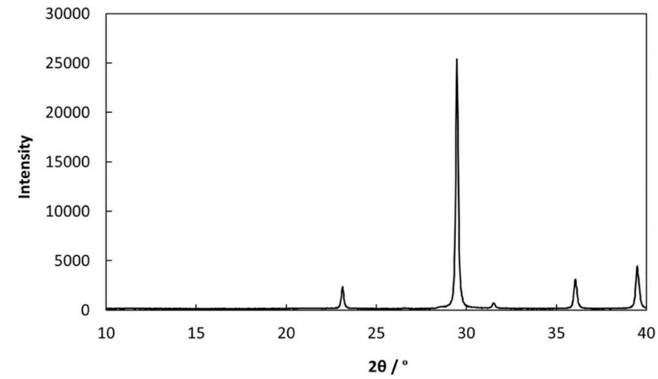

Fig. 4. XRD pattern of f-$CaCO_3$ nanoadditives.

2.2. Nanoadditives

Regarding the nanoparticles used as additives of castor and soybean base oils, functionalized calcium carbonate nanoparticles, f-$CaCO_3$, were chosen (from US Research Nanomaterials, Houston, USA). f-$CaCO_3$ NPs coated with fatty acid have 98 % purity and a 40–80 m^2/g specific surface area according to the supplier. These NPs were fully characterized using several characterization techniques. Therefore, f-$CaCO_3$ nanoparticles have been characterized through infrared spectroscopy (FTIR) and Raman spectroscopy to establish the bonds related with f-$CaCO_3$ NPs (Fig. 3). The FTIR spectrum of the f-$CaCO_3$ NPs (Fig. 3a) shows three pronounced peaks placed at 710 cm^{-1}, 870 cm^{-1} and 1450 cm^{-1} consistent to deformation in plane, deformation outside in-plane and doubly degenerate in-plane strain typical of $CaCO_3$, respectively. [42,43]. Furthermore, it can be also observed that around 2900 cm^{-1} some peaks are present due to the fatty acid functionalization [44]. Besides, the Raman spectrum of f-$CaCO_3$ (Fig. 3b) displays a band around 710 cm^{-1} that corresponds to E_g phonon, a strong Stokes band around 1100 cm^{-1} that coincides with A_{1g} phonon, and a another weak band at 1430 cm^{-1} that corresponds to another E_g phonon[45,46].

Furthermore, f-$CaCO_3$ NPs were characterized using X-Ray diffraction to verify its crystalline pattern. Thus, a D8 Advance from Bruker (Massachusetts, USA) with Cu-Kα radiation (λ = 1.5418 nm) was employed. The XRD study was completed between 2θ= 10–40°. Additionally, the Debye-Scherrer's equation was used to estimate the size of

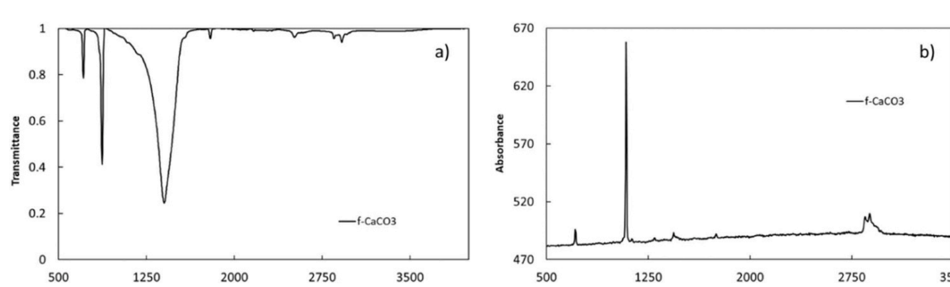

Fig. 3. FTIR (a) and Raman (b) spectrum of f-$CaCO_3$ nanopowders.

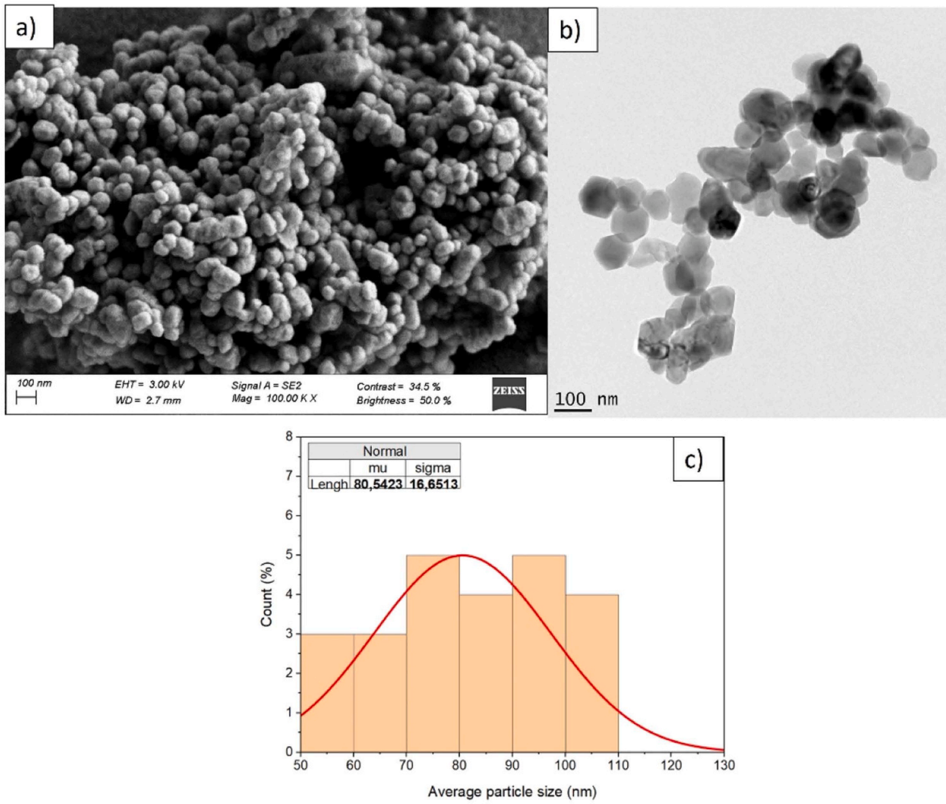

Fig. 5. SEM (a) and TEM (b) images and size nanoparticles distribution (c) of f-$CaCO_3$ nanopowders.

the NPs based on the subsequent formula [47]:

$$Dp = K\,\lambda\,/\,(\beta\cos\theta) \tag{1}$$

where *Dp* is the mean crystallite size (nm), *K* the Scherrer constant, *λ* the whole width at the half summit of the diffraction peak, β denotes the full width at half maximum (FWHM) and θ the Bragg angle of the peak. Fig. 4 displays the XRD pattern of f-$CaCO_3$ NPs. It can be observed that peaks are placed at 2θ= 22.9°, 29.34°, 36.11° and 39.45°, corresponding to (012), (104), (110), (113) crystal planes [48]. Thus, this experimental XRD investigation matches with the ICSD Card of Calcite (No: 98–004-0107) [48]. The $CaCO_3$ NPs crystallite size calculated using the aforementioned Eq. 1 is 86.7 nm.

Finally, f-CaCO3 NPs were also characterized by means of Scanning electron microscopy, SEM, (FESEM Ultra Plus from Zeiss, Jena, Germany) and transmission electron microscopy, TEM, (1011 from JEOL. Tokyo, Japan) methods in order to know their morphology and size. It must be noted that through TEM image (Fig. 5b) and using Image J software the average particle size was calculated. SEM and TEM images (Figs. 5a and 5b) reveal that the studied f-CaCO3 NPs exhibit an almost spherical shape. Furthermore, the obtained average size of NPs was around 80 nm (Fig. 5c). This average size is similar to that obtained with XRD characterization (86.7 nm).

2.3. *Formulation and stability of potential green nanolubricants*

To formulate the nanodispersions of castor oil and soybean oil with functionalized $CaCO_3$ NPs, the typical two-step process was performed [49]. Hence, the following eight potential nanolubricants were prepared by utilizing a MC 210 P Sartorius balance (0.01 mg readability):

Castor Oil + (0.05 wt% f-$CaCO_3$, 0.10 wt% f-$CaCO_3$, 0.15 wt% f-$CaCO_3$, 0.20 wt% f-$CaCO_3$).

Soybean Oil + (0.05 wt% f-$CaCO_3$, 0.10 wt% f-$CaCO_3$, 0.15 wt% f-$CaCO_3$, 0.20 wt% f-$CaCO_3$).

The main reason to choose these mass concentrations (0–0.20 wt%)

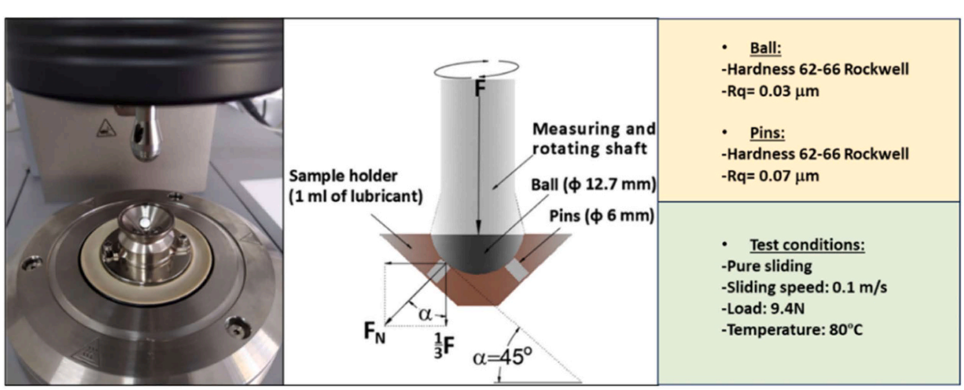

Fig. 6. Ball-on-three pins configuration and tribological details.

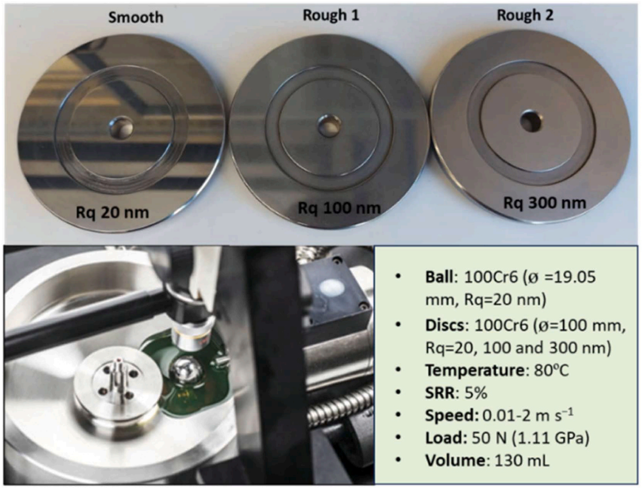

Fig. 7. Rolling-sliding tribometer configuration and tribological details of specimens.

was the good tribological performances obtained in previous studies of nanoparticles as lubricant additives [43,50]. After the preparation, the aforementioned nanolubricants were agitated during 3 h via ultrasonic bath working in continuous mode to obtain homogeneous nanodispersions. The stability against sedimentation of the prepared nanodispersions was examined through two different methods: visual control and refractometry. The former is a qualitative process, in which the nanodispersions are photographed each 24 h observing if the NPs are deposited or not. Regarding the latter, the refractive index evolution over time of nanolubricants is studied with the aim of quantifying the precipitation of NPs. For this task, a Metler Toledo refractometer was utilized [51].

2.4. Tribological characterization under pure sliding conditions

Tribological analyses were performed with the two base oils, Castor oil and Soybean oil, and their formulated f-$CaCO_3$ nanolubricants (0.05 wt%, 0.10 wt%, 0.15 wt% and 0.20 wt% f-$CaCO_3$) to examine if these nanoadditives present antifriction and/or antiwear properties. For this purpose, a rheometer of Anton Paar (Graz, Austria), MCR 302, set up with a T-PTD200 tribology unit was utilized in ball-on-three pins disposition, being the ball situated on a tube and pins are set into a circular box (Fig. 6). Friction pure sliding tests were performed at 213 rpm rotational speed (0.1 m s^{-1} at the contact points) and 9.4 N load in each pin implying a maximum Hertzian pressure of 1.1 GPa, a duration of 3400 s and a temperature of 353.15 K. Pins are flooded after inserting around 1 mL of lubricant. Besides, three different trials were performed for each lubricant sample. More descriptions considering this device can be found in previous research [52].

After performing the friction analyses described previously, wear is generated in the pins. Therefore, to evaluate the produced wear and compare between base oils and nanolubricants, pins were analyzed through an optical profilometer Sensofar S-Neox to obtain information about the different wear indicators, wear scar diameter (WSD), wear track depth (WTD) and worn area, and about the roughness inside the worn surfaces employing the ISO4287 standard with a Gaussian filter (cut-off: 0.08 mm). Likewise, to examine the surfaces of worn pins and obtain knowledge concerning the nanolubricants elements in worn areas (base oil and NPs) and possible tribological mechanisms that could act, a Raman microscope WITec alpha300R+ was utilized to obtain raman mappins of worn surfaces. Finally, SEM characterization of worn surfaces was also carried out to improve the information concerning the tribological mechanisms.

2.5. Tribological characterization under rolling-sliding conditions

A tribometer EHD2 (PCS Instruments, UK) with a ball-on-disc disposition, was utilized to perform friction tests of a metal contacts formed by a ball and a rotational disc (Fig. 7). Both components are driven with two different electric motors to perform the rolling-sliding tests. The test conditions are also summarized in Fig. 7. More information concerning this apparatus can be seen in previous research [53]. These kind of tests were completed for the castor and soybean base oils and their respective optimal f-$CaCO_3$ nanolubricants with the greatest tribological performance reached in pure sliding tests. Thus, Stribeck curves were obtained for the base oils and f-$CaCO_3$ nanolubricants using three different discs (one smooth and two rough, Fig. 7) for a 5 % slide-to-roll ratio (SRR) [53]. Friction coefficient is established like the mean of those achieved from two individual tribological tests, the first ramp speed increasing speed and the second one reducing speed.

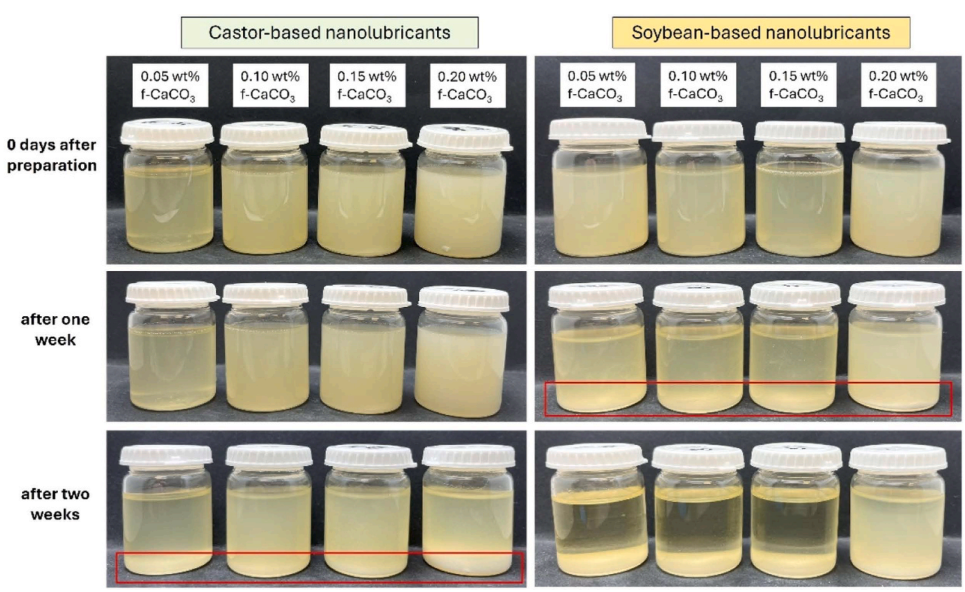

Fig. 8. Visual stability of castor and soybean based nanolubricants.

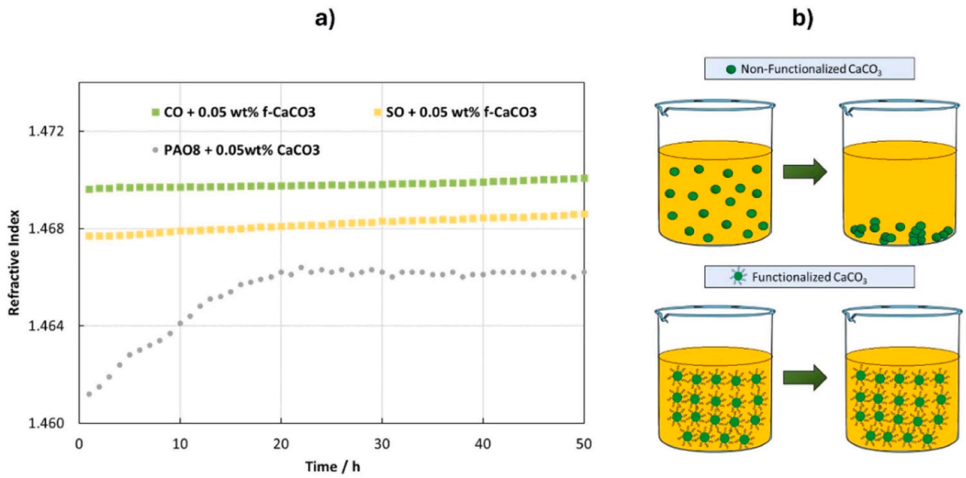

Fig. 9. Refractive index evolution (a) and schematic representation of coated and uncoated NPs in terms of stability (b).

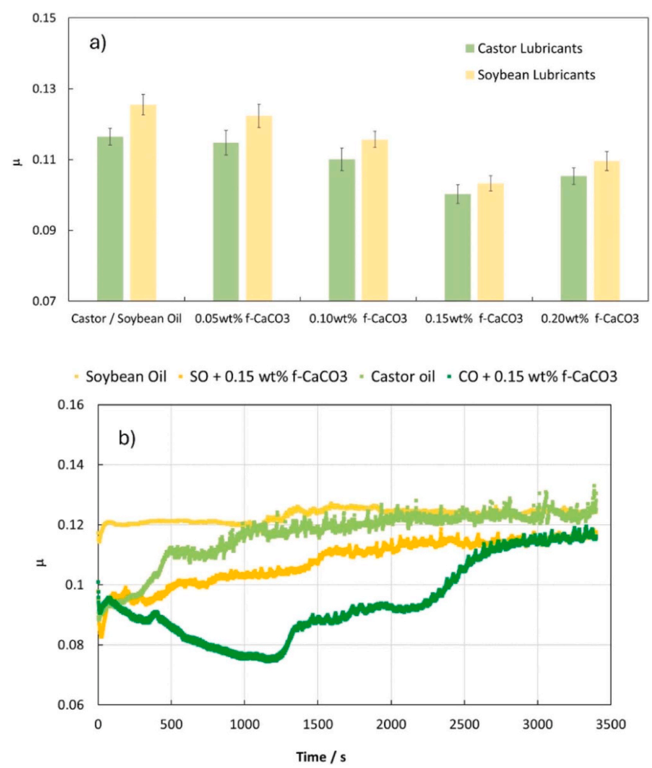

Fig. 10. Mean friction coefficients (μ) found with Castor and soybean base oils and their f-$CaCO_3$ nanolubricants (a) and their behavior during time (b).

3. Results

3.1. Nanolubricants stability

The stability against sedimentation of f-$CaCO_3$ nanolubricants based on castor oil and soybean oil was investigated qualitatively via visual observation and quantitative by means of refractometry technique. As Fig. 8 reveals, for the castor-based nanolubricants the sedimentation appears after two weeks of homogenization, while for the soybean-based nanolubricants, the sedimentation appears after the first week of sonication, therefore better visual stability was observed for the castor nanolubricants. This fact may be owing to the higher viscosity of castor oil in comparison to soybean oil.

Regarding the refractometry, Fig. 9a presents the refractive index progress during time for the f-$CaCO_3$ nanolubricants based on castor and soybean oils, in order to quantify the importance of presenting a fatty acid functionalization in the NPs. As it can be observed, the sedimentation rate for both type of nanolubricants is quite slow. Precisely, after 50 h the variation of refractive index was 0.03 % and 0.06 % for castor and soybean nanolubricants, respectively. These results indicate a very good stability against sedimentation for the used NPs in comparison to another previous research work [43] that uses uncoated $CaCO_3$ NPs. As it is presented in Fig. 9a, the stability for uncoated $CaCO_3$ nanolubricants is quite worse than that obtained for the f-CaCO3 nanolubricants. Specifically, for the uncoated nanolubricants the variation of refractive index was 0.19 % after only 10 h. Thus, it can be observed that through the functionalization of NPs, the stability of nanolubricants is improved (Fig. 9b).

3.2. Friction and wear results in pure sliding

As it was mentioned previously, friction tests with castor and

Table 3
Attained mean friction coefficients, μ, and wear parameters (WSD, WTD and Area) with standard deviations, σ, for the Castor and Soybean lubricants at 353.15 K.

Lubricant	μ	σ	WSD/μm	σ/μm	WTD/μm	σ/μm	Area/ μm^2	σ/ μm^2
Castor Oil	0.117	0.002	425	21	3.2	1.1	975	220
+ 0.05 wt% f-$CaCO_3$	0.115	0.003	398	17	3.0	1.3	892	211
+ 0.10 wt% f-$CaCO_3$	0.110	0.003	363	23	3.1	1.3	731	126
+ 0.15 wt% f-$CaCO_3$	0.100	0.003	291	16	1.6	1.0	392	102
+ 0.20 wt% f-$CaCO_3$	0.105	0.002	370	31	2.8	1.2	690	126
Soybean Oil	0.126	0.003	525	21	4.6	0.7	1387	380
+ 0.05 wt% f-$CaCO_3$	0.122	0.003	508	17	3.8	0.8	1281	231
+ 0.10 wt% f-$CaCO_3$	0.115	0.002	423	15	2.8	0.6	860	197
+ 0.15 wt% f-$CaCO_3$	0.103	0.002	398	18	2.3	0.5	603	112
+ 0.20 wt% f-$CaCO_3$	0.109	0.003	414	21	2.4	0.4	671	110

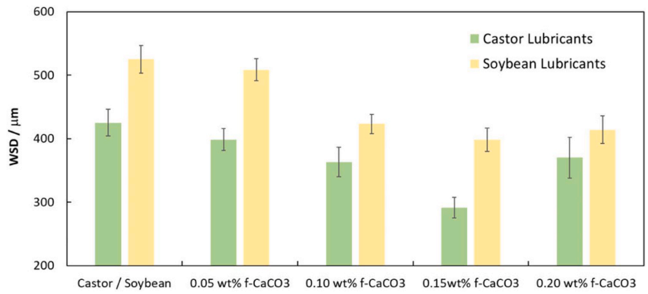

Fig. 11. Wear scar diameters (WSD) found with Castor and soybean base oils and their f-$CaCO_3$ nanolubricants.

soybean oils and with their corresponding f-$CaCO_3$ nanolubricants were performed, being the obtained values presented in Fig. 10a and Table 3. As it can be observed, for both kind of f-$CaCO_3$ nanolubricants (based on castor and soybean oils), the reached friction coefficients are quite smaller than those attained with the base oils. Thus, the greatest friction reductions were achieved for the 0.15 wt% f-$CaCO_3$ nanolubricants for both castor and soybean-based lubricants. In particular, maximum friction decreases of 14 % and 18 % were achieved compared to castor and soybean base oils, respectively. As it can be observed in Fig. 10a, friction coefficients decrease gradually from as the mass concentration of NPs increases, until reaching a bottom at the 0.15 wt% f-$CaCO_3$ (optimal performance) to then increase the friction behavior at the highest mass concentration of NPs (0.20 wt%). This singularity might be owing to very low mass concentrations the quantity of NPs is not enough to achieve a suitable friction performance and when the concentration is high (0.20 wt%), NPs are more expected to agglomerate in friction tests, being difficult for NPs to enter the tribological contact, producing inferior lubrication capacity. So, the produced aggregates as impurities can scratch the friction surface and consequently the friction rises. Furthermore, it is observed that soybean base oil and nanolubricants have a higher friction coefficient in comparison to castor oil lubricants. This fact may be due to the higher viscosity of castor oil in comparison to soybean oil. Finally, friction performance for castor and soybean base oils and nanolubricants with greatest performance during time can be observed in Fig. 10b.

After completing the aforementioned friction tests, the used pins presented wear. As displayed in Fig. 11 and Table 3, the wear generated in pins lubricated with f-$CaCO_3$ nanolubricants is much smaller than those created with castor and soybean base oils, showing the NPs excellent antiwear properties. It is clear that the optimal mass concentration for castor and soybean nanolubricants was the intermediate concentration of 0.15 wt% with WSD reductions of 27 % and 24 % compared to base oils. Concerning of worn area, maximum reductions of 35 % and 56 % were achieved for the 0.15 wt% optimal nanolubricants, in comparison to castor and soybean base oils. Fig. 12 displays the important wear reductions of optimal nanolubricants in comparison with castor base oil (Fig. 12a) and soybean base oil (Fig. 12b). Therefore, outstanding reductions in wear were achieved through the addition of f-$CaCO_3$ NPs to the castor and soybean oils.

Additionally, roughness analyses on pins obtained after friction tribological tests reveal that the tested worn pins with f-$CaCO_3$ nanolubricants have less roughness than those achieved with the two base oils (Table 4). Hence, a Ra value of 33.6 and 35.8 nm were found for the worn pins lubricated with castor and soybean oils, respectively. On the other hand, pins with the optimal castor and soybean nanolubricants (0.15 wt% f-$CaCO_3$) reached the minimal Ra values (20.6 and 19.3 nm, respectively) indicating a remarkable roughness decreases around 40 % and 45 %, correspondingly. These results imply that owing to the f-$CaCO_3$ addition to base oils, a more regular worn surface is detected after pure sliding tests. For better visualization of roughness, the surface roughness images, and roughness profiles are presented in Fig. 13.

Raman mappings of the worn surfaces after friction studies were performed to investigate the distribution of the NPs in the worn tracks and how they can participate in the remarkable friction and wear improvements of nanolubricants. Previously, each Raman spectrum of

Table 4
Mean roughness values, Ra and Rq in worn pins examined with the f-$CaCO_3$ nanolubricants and base oils.

Lubricant	Ra/nm	σ	Rq/ nm	σ
Untested Pin	50.1	3.9	59.6	4.8
Castor oil	33.6	2.8	42.5	3.2
+ 0.05 wt% f-$CaCO_3$	28.8	2.6	32.7	3.3
+ 0.10 wt% f-$CaCO_3$	22.9	1.5	25.0	1.5
+ 0.15 wt% f-$CaCO_3$	20.6	2.3	23.2	2.1
+ 0.20 wt% f-$CaCO_3$	24.3	1.7	27.2	1.6
Soybean oil	35.8	3.1	39.4	4.5
+ 0.05 wt% f-$CaCO_3$	27.2	2.4	30.4	3.0
+ 0.10 wt% f-$CaCO_3$	24.5	2.2	27.9	2.4
+ 0.15 wt% f-$CaCO_3$	19.3	1.6	22.9	2.1
+ 0.20 wt% f-$CaCO_3$	24.1	2.3	27.2	2.3

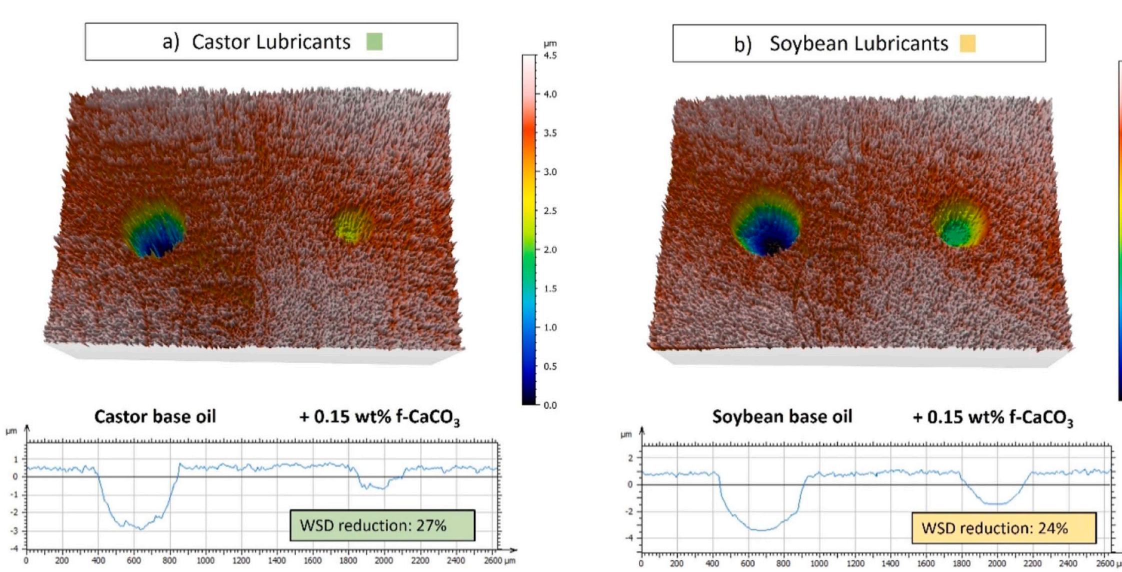

Fig. 12. Comparison between 3D profiles found with castor (a) and soybean (b) base oils and their optimal f-$CaCO_3$ nanolubricants.

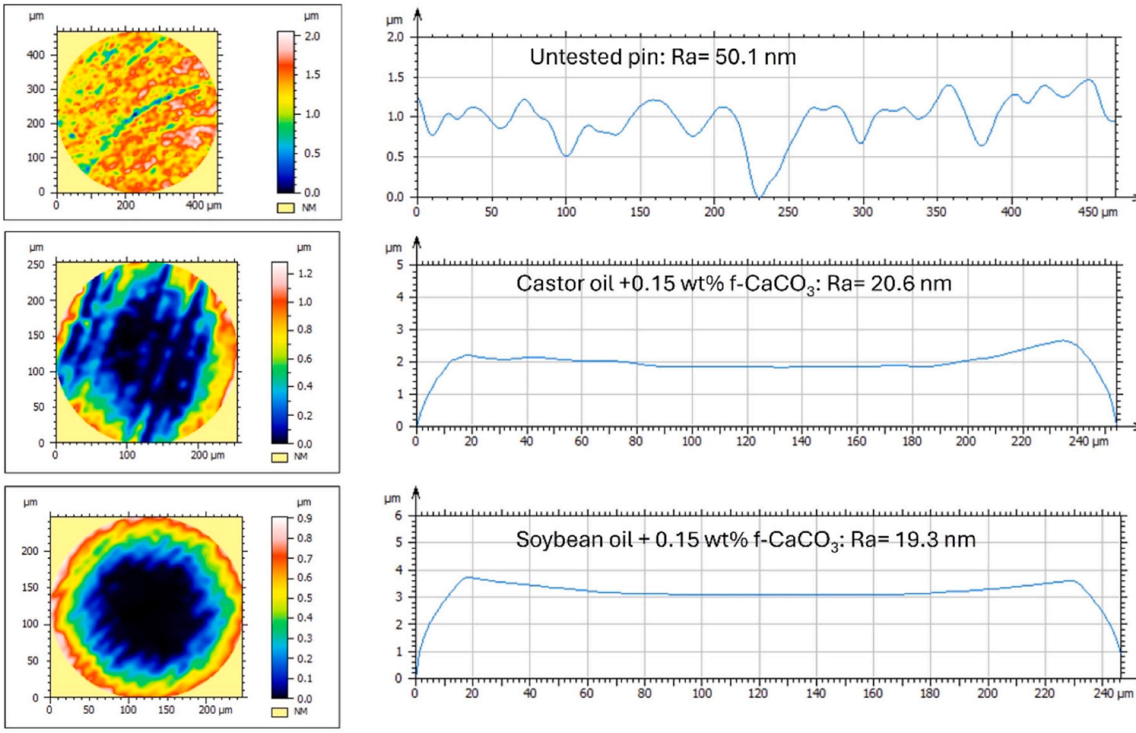

Fig. 13. Surface roughness and roughness profiles observed for untested and tested metallic samples.

nanolubricants components were presented: castor and soybean oils (Fig. 2) and f-$CaCO_3$ (Fig. 3b) to recognize the elements in Raman mappings. Two mappings were performed to observe the worn pins tested with the castor and soybean nanolubricants with the optimal anti-wear behavior (0.15 wt% f-$CaCO_3$ for both base oils), Fig. 14. Regarding the castor nanolubricant, Fig. 14a, it presents the areas in blue and green, matching the peaks of the spectrum with those achieved for castor oil and f-$CaCO_3$ NPs, respectively. Similarly, for soybean nanolubricant, Fig. 14b, it also presents the areas in blue and green, coincide the peaks of the spectrum with those attained for soybean oil and f-$CaCO_3$ NPs, respectively. It is also observed that in the case of mapping with soybean nanolubricants, the spots of f-$CaCO_3$ have a lower size and are quite better distributed in the worn surface, in comparison with mapping of castor nanolubricants. This fact can be a possible reason for obtaining a greater roughness reduction in comparison to base oils. Thus, for both mappings (castor and soybean nanolubricants), considering the presence of f-$CaCO_3$ Raman spectrum in worn surfaces it is clearly observed that f-$CaCO_3$ are trapped in the metal contact and fill in the gap between the rubbing surfaces facilitating the decrease of friction and wear through prevent direct metal-metal contact. The deposits of f-$CaCO_3$ NPs are placed in the sliding direction and could form a protective layer of low shear strength on the worn surface that enhances the lubrication performance of castor and soybean base lubricants. The greater surface energy of NPs permits them to chemically react with the rubbing surfaces to produce a tribofilm, which can minimize direct contact with the steel surfaces. Considering these observations and the improved roughness values (Table 3) for the f-$CaCO_3$ nanolubricants it can be observed that formation of tribofilm and repairing mechanism (filling the NPs the valleys in the contact surfaces) played on the worn surface during tribological tests. Additionally, as the NPs present a spherical shape, the rolling-bearing mechanism could also be present in the reduction of friction and wear by changing the sliding friction between the rubbing surfaces to rolling friction. Similar results were observed by Sunqing et al. [35] who investigated the tribological characteristics of $CaCO_3$ NPs as 500SN base oil. They observed that $CaCO_3$ NPs have decomposed to CaO during tribological tests, and a film formed by $CaCO_3$ and CaO was created on the contact surfaces. They concluded that the tribological mechanisms are the tribofilm formation and rolling-bearing. Furthermore, Zhang et al. [36] studied the antiwear properties of $CaCO_3$ NPs as additives of PAO10 base oil. These authors found that the tribological mechanism is ascribed completely to the deposition of $CaCO_3$ NPs, with the creation of CaO from $CaCO_3$ and other elements on the worn metal surface.

In order to improve the information regarding the tribological mechanism, SEM characterization of untested pin (Fig. 15a) and worn surfaces tested with castor and soybean base oils (Fig. 15b and Fig. 15c) and their optimal nanolubricants in friction and wear: castor oil + 0.15 wt% f-$CaCO_3$ (Fig. 15d) and soybean oil+ 0.15 wt% f-$CaCO_3$ (Fig. 15e), were performed. As it can be observed in Fig. 15b and Fig. 15c, critical adhesive wear and plastic deformation just occurred on the steel surface when the base oils were used as lubricants, as proved by the formation of deep furrows. Nevertheless, in the lubrication with castor and soybean oils containing f-$CaCO_3$ NPs (Fig. 15d and Fig. 15e), the sliding surfaces were quite smooth and critical wear did not appear. These facts suggest that a tribofilm consisting of f-$CaCO_3$ NPs and the organic compounds from the NPs modifier (fatty acid) was created.

To sum up, considering the roughness analyses, Raman mapping and SEM observations of worn surfaces, it was resolved that the tribological mechanisms are the tribofilm formation, repairing mechanism and rolling-bearing mechanism due to the spherical shape of NPs. Thus, these tribological mechanisms are schematically described in Fig. 16.

3.3. *Tribological results in rolling-sliding*

Tribological rolling-sliding test for castor and soybean base oils and their respective opimal nanolubricants in pure sliding conditions (0.15 wt% f-$CaCO_3$) were carried out at operating temperature of 80 ºC and SRR of 5 % reaching the friction characterization through Stribeck Curves (Fig. 17). The Stribeck curves is the result of plotting the coefficient of friction versus specific film thickness, Λ, which is calculated by: $\Lambda = \frac{h_t}{Rq}$, where h_t is the theoretic film thickness and Rq is the composite roughness of tribological pairs: $Rq = \sqrt{(Rq_{disc})^2 + (Rq_{ball})^2}$. The h_t

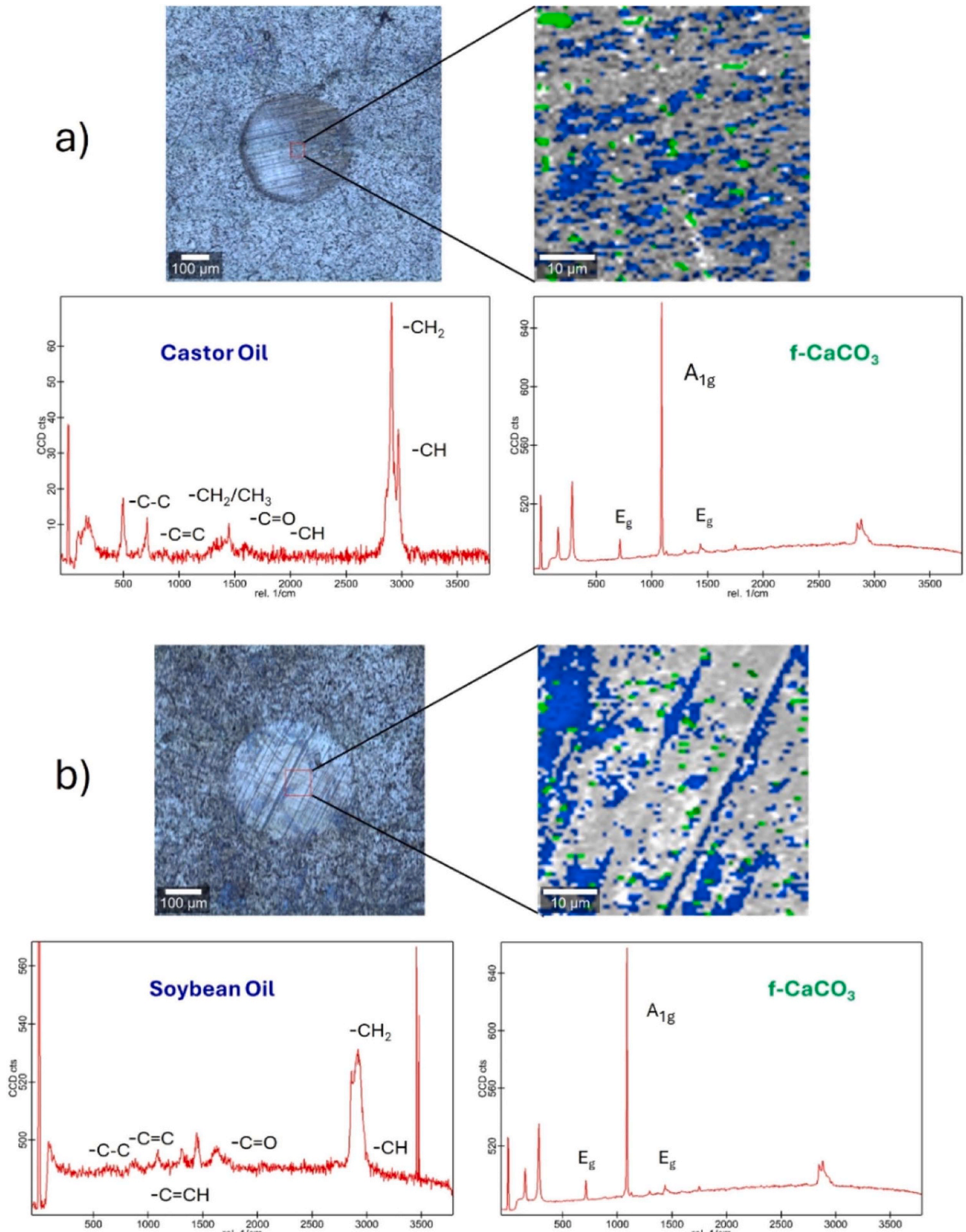

Fig. 14. Mapping Raman of surfaces tested with optimal castor (a) and soybean (b) nanolubricants.

at the 80 °C temperature was guessed with the Hamrock and Downson's equation [54], contemplating diverse factors such as materials and lubricant properties or working conditions. For the approximation of h_t, the trimethylpropane trioleate base oil pressure−viscosity coefficient was employed [55]. Besides, a Stabinger SVM 3000 (Anton Paar, Austria) was employed to measure the dynamic viscosities up to 100 °C (Table S1).

The achieved Stribeck curves are plotted in Fig. 17a for castor and Fig. 17b for soybean base oils and their optimal f-$CaCO_3$ nanolubricants using three discs with different roughness (0.02, 0.10 and 0.30 Rq). As it can be seen in the graphs, for both kind of lubricants (castor and soybean) important friction reduction happens owing to the addition of f-$CaCO_3$, especially at low speeds with the roughest disc. Nonetheless, it is also observed that the additived and non-additived lubricants behave similarly with the two smoothest discs and with the roughest disc for speeds above 500–700 mm/s. In these conditions the specific film thickness is quite thick which decreases the synergetic effects of the nanoparticles that are thought to be effective under boundary conditions. As the speed decreases, the direct contact between asperities start to occur and the inclusion of the nanoparticles decrease the coefficient of friction under rolling-sliding conditions. Thus, for small speeds the outcome of the f-$CaCO_3$ NPs addition is essential, with outstanding friction reductions when the hydrodynamic impact is minor (low speeds), therefore operating the NPs successfully at boundary conditions. The reached results are quite attractive for oil engine and gears applications, regularly operating at elevated temperatures [56].

Commonly, a Stribeck curve is divided in various lubrication regimes: boundary, mixed, elastohydrodynamic (EHL) and full film lubrication (FFL). Varying on the diverse criteria in literature, boundary regime appears when $\Lambda < 1$, mixed if $1 < \Lambda < 3$, EHL while $\Lambda > 3$ and with $\Lambda > 5$, FFL. Thus, in these rolling-sliding tests Λ values vary between a minimum over 0.04 (for the soybean lubricants with roughest disc) to about 13.9 (for the castor lubricants with smoothest disc). Accordingly, following the aforementioned classification, boundary lubrication occurs for all the examined discs (0.02, 0.10 and 0.30 Rq) except for the smoothest disc (0.02 Rq) with castor-based lubricants,

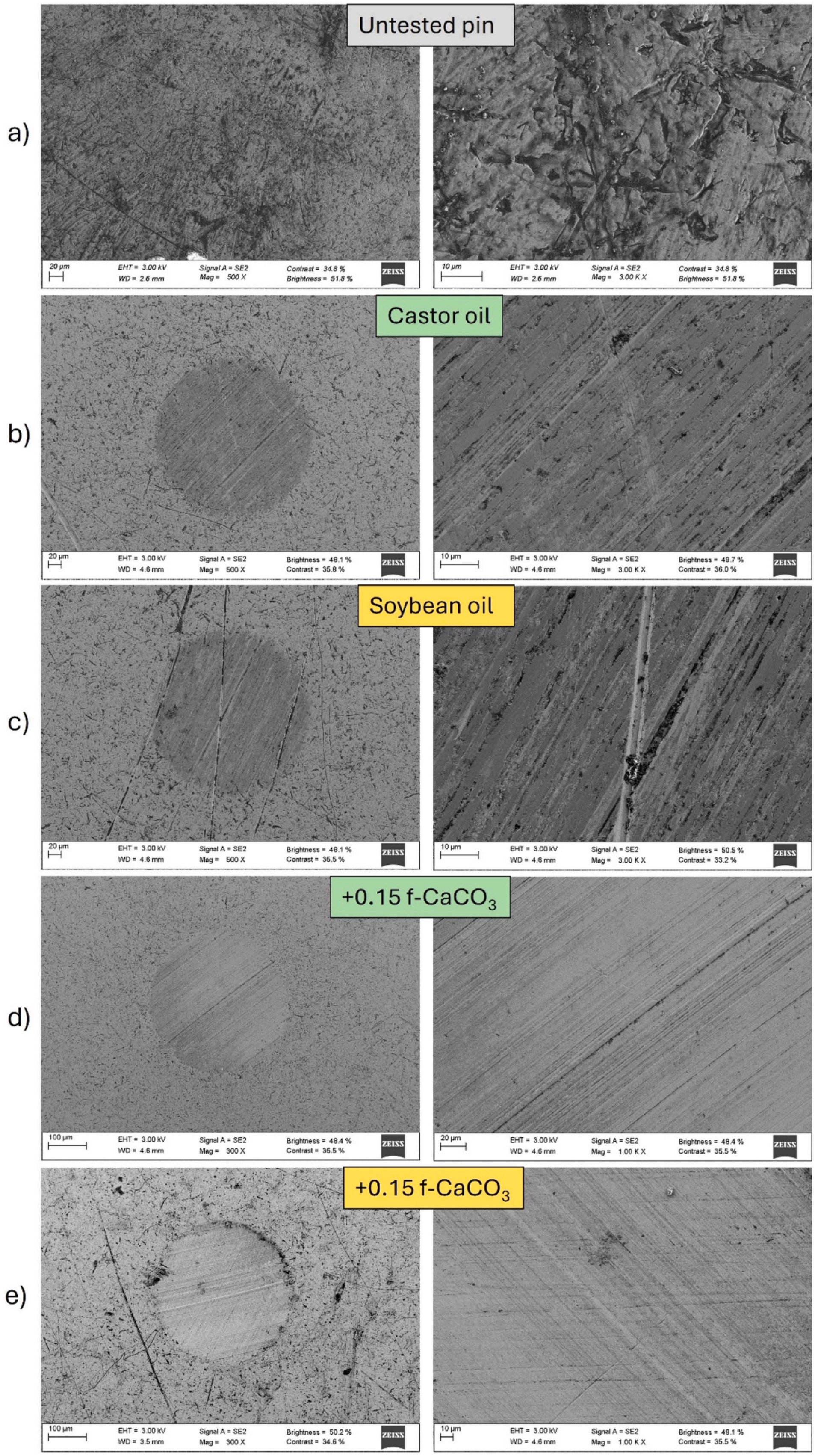

Fig. 15. SEM images of untested pin (a) and worn pins tested with castor (b) and soybean (c) base oils and optimal castor (d) and soybean (e) nanolubricants.

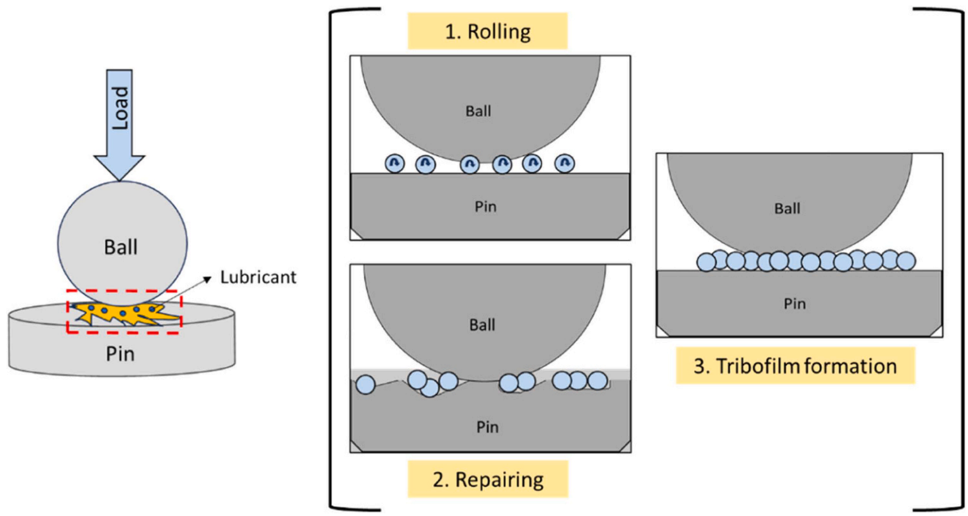

Fig. 16. Schematic representation of the possible tribological mechanisms.

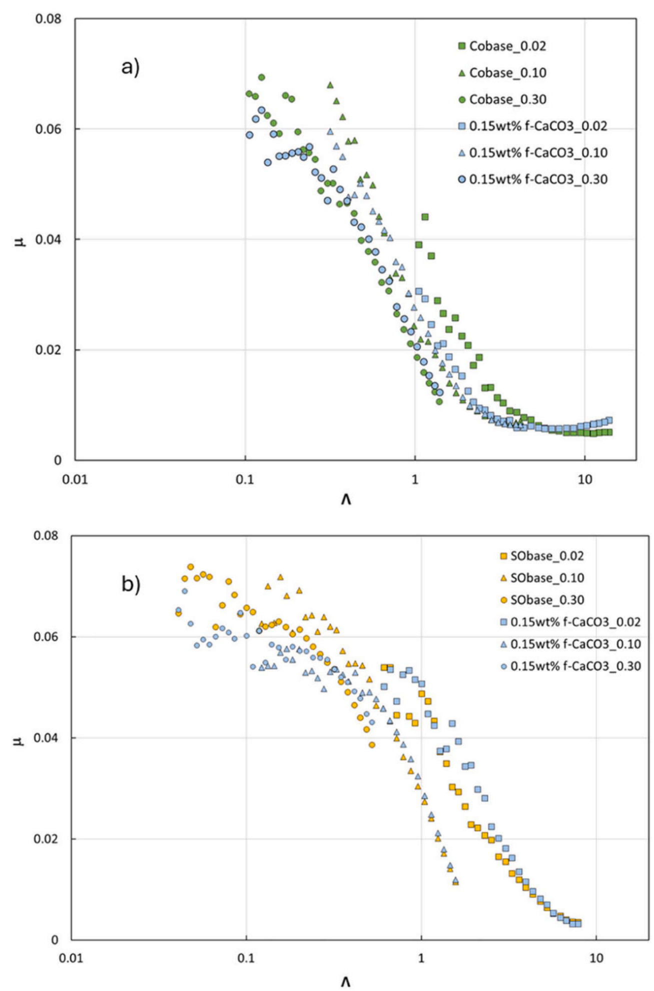

Fig. 17. Full Stribeck curves reached with castor oil (a), soybean oil (b)and their f-$CaCO_3$ nanolubricants (a and b).

mixed lubrication happens for all discs with castor lubricants and the two smoothest discs (0.02 and 0.10 Rq) with soybean lubricants whereas EHL and FFL occurs for the two smoothest discs (0.02 and 0.10 Rq) with castor-based lubricants and with the smoothest disc (0.02 Rq) for soybean-based lubricants. Therefore, a full friction characterization in all the lubricant regimes were performed through rolling-sliding tests.

4. Current challenges and future considerations

The market penetration of biolubricants has been limited in many applications. This is likely due to their poor oxidative stability and their inferior properties at lower temperatures. The principal obstacle is the high degree of variability and seasonality of the feedstock, which gives rise to different chemical compositions of the starting vegetable oil [57]. Another challenge is the selection of the non-edible oil. Different research have been conducted with vegetable oils that could potentially disrupt the food chain, including sunflower, soybean, and palm oil, among others [57]. The use of these oils could potentially lead to price speculation and social differences. As a consequence, the promotion of non-edible oils, as jojoba oil and castor oil, has increased significantly over recent years as a green alternative [58]. Furthermore, microalgae have developed as a potential source of biodegradable oil owing to its high oil content, which has been observed to exceed 70 % [59]. The future of biolubricants should focus on the development of lubrication properties and ecotoxicity that are enhanced to those of conventional mineral oils. The development of more sustainable formulations is required in fields that include engine oils and hydraulic oils, among others. Regarding the economic issue, it is needed to identify reliable and cheap vegetable oils as starting materials making efforts in chemically modifying the preliminary vegetable oils to enhance the formulation of desired biolubricants. For this purpose, the lubricant-synthesizing companies should change their production chains in order to develop these lubricants efficiently, although it is evident that this process requires a huge investment and time. Regarding the use of nanolubricants, one of the main challenges for the tribology researchers, engineers and end users is recycle and reuse the nanolubricants components. As Kimura et al. [60] reported, near 30 % of lubricant oils in advanced countries is wasted, which relatively contaminate the global environment. Hence, applying a suitable recyclability process would reduce the overall cost of a nanolubricant, being economically feasible.

5Conclusions

In this research, the following conclusions were found:

– Eco-friendly nanolubricants were formulated using castor and soybean oils additived with functionalized $CaCO_3$ nanoparticles (f-

$CaCO_3$) observing time stabilities around two weeks castor nanolubricants and one week for soybean nanolubricants.
- Friction coefficients achieved in pure sliding conditions with f-$CaCO_3$ nanolubricants are lower than those attained for castor and soybean base oils with reductions of 14 % and 18 %, respectively, for an optimal concentration of 0.15 wt% f-$CaCO_3$.
- Important wear improvements in pins tested with f-$CaCO_3$ nanolubricants were observed in comparison with those tested base oils, reaching maximum decreases of 27 % and 24 % compared to castor and soybean base oils for the 0.15 wt% f-$CaCO_3$ nanolubricants.
- Based on the NPs shape, roughness analysis, Raman microscopy and SEM of worn surfaces, it is suggested that the lubrication mechanism is explained by rolling effect, the adsorbed tribofilm and repairing.
- Relating the rolling–sliding tests, f-$CaCO_3$ NPs play a decisive role in the maximum boundary lubrication regime, substantially lowering the friction coefficient.
- This research reveals the benefit of using $CaCO_3$ NPs and castor or soybean oils in the field of tribology, being the special importance the good tribological performance for castor nanolubricants for the nature of a non-edible oil.
- High-performance $CaCO_3$-based nanolubricants seem to be a commercially feasible alternative to conventional and harmful petroleum-based lubricants.

Statement of Originality

The authors declare that the work described in this manuscript has not been published previously by any of the authors, that it is not under consideration for publication elsewhere, that its publication is approved by all authors and tacitly or explicitly by the responsible authorities where the work was carried out, and that, if accepted, it will not be published elsewhere in the same form, in English or in any other language, including electronically without the written consent of the copyright holder.

CRediT authorship contribution statement

Jorge H.O. Seabra: Writing – review & editing, Project administration, Funding acquisition, Conceptualization. **David E.P. Gonçalves:** Writing – review & editing, Methodology. **Carlos M.C.G. Fernandes:** Writing – review & editing, Methodology, Investigation. **Jose Manuel Liñeira del Rio:** Writing – review & editing, Writing – original draft, Methodology, Investigation, Conceptualization.

Declaration of Competing Interest

The authors declare that they have no known competing financial interests or personal relationships that could have appeared to influence the work reported in this paper.

Data Availability

Data will be made available on request.

Acknowledgments

This research is supported by Xunta de Galicia (ED431C 2020/10) and by LAETA, Portugal under project UID/50022/2020. JMLdR is grateful for financial support through the Margarita Salas program, funded by MCIN/AEI/10.13039/501100011033 and "NextGenerationEU/PRTR". Furthermore, authors are also thankful to RIAIDT-USC for its analytical facilities.

Appendix A. Supporting information

Supplementary data associated with this article can be found in the online version at doi:10.1016/j.triboint.2024.110007.

References

[1] Benedicto E, Rubio EM, Aubouy L, Sáenz-Nuño MA. Sustainable lubrication/cooling systems for efficient turning operations of γ-tial parts from the aeronautic industry. Int J Precis Eng Manuf-Green Technol 2023;10:709–28. https://doi.org/10.1007/s40684-022-00435-x.
[2] Kumar B. Oil and lubricant hazard effects on human health. Int J Innov Sci, Eng Technol 2017;4:315–22.
[3] Zheng T, Fang J, Xie Q, Wu Z, Lu M, Xia F, et al. Measurement and correlation of the density, viscosity and vapor pressure of fatty acid 2-ethyhexyl esters. J Chem Thermodyn 2019;130:243–50. https://doi.org/10.1016/j.jct.2018.10.012.
[4] Garcés R, Martínez-Force E, Salas JJ. Vegetable oil basestocks for lubricants. Grasas Y Aceites 2011;62:21–8. https://doi.org/10.3989/gya.045210.
[5] Nagendramma P, Kaul S. Development of ecofriendly/biodegradable lubricants: an overview. Renew Sustain Energy Rev 2012;16:764–74. https://doi.org/10.1016/j.rser.2011.09.002.
[6] Dalbey WE, Biles RW. Respiratory toxicology of mineral oils in laboratory animals. Appl Occup Environ Hyg 2003;18:921–9. https://doi.org/10.1080/10473220390237548.
[7] Kurre SK, Yadav J. A review on bio-based feedstock, synthesis, and chemical modification to enhance tribological properties of biolubricants. Ind Crops Prod 2023;193:116122. https://doi.org/10.1016/j.indcrop.2022.116122.
[8] Kim H, Choi N, Kim Y, Kim H-R, Lee J, Kim I-H. Immobilized lipase-catalyzed esterification for synthesis of trimethylolpropane triester as a biolubricant. Renew Energy 2019;130:489–94. https://doi.org/10.1016/j.renene.2018.06.092.
[9] Miller SA, Landis AE, Theis TL, Reich RA. A comparative life cycle assessment of petroleum and soybean-based lubricants. Environ Sci Technol 2007;41:4143–9. https://doi.org/10.1021/es062727e.
[10] Mousavi SB, Heris SZ, Estellé P. Experimental comparison between ZnO and MoS2 nanoparticles as additives on performance of diesel oil-based nano lubricant. Sci Rep 2020;10:5813. https://doi.org/10.1038/s41598-020-62830-1.
[11] Mousavi SB, Zeinali Heris S. Experimental investigation of ZnO nanoparticles effects on thermophysical and tribological properties of diesel oil. Int J Hydrog Energy 2020;45:23603–14. https://doi.org/10.1016/j.ijhydene.2020.05.259.
[12] Ali ZAAA, Takhakh AM, Al-Waily M. A review of use of nanoparticle additives in lubricants to improve its tribological properties. Mater Today: Proc 2022;52:1442–50. https://doi.org/10.1016/j.matpr.2021.11.193.
[13] Gulzar M, Masjuki HH, Kalam MA, Varman M, Zulkifli NWM, Mufti RA, et al. Tribological performance of nanoparticles as lubricating oil additives. J Nanopart Res 2016;18:223. https://doi.org/10.1007/s11051-016-3537-4.
[14] Bharat N, Bose PSC. Optimization of tribological behaviour of TiO2 nanoparticles reinforced AA7178 alloy matrix using ANN and Taguchi's methodology. Surf Topogr: Metrol Prop 2022;10. https://doi.org/10.1088/2051-672X/ac7a55.
[15] Bharat N, Bose PSC. Microstructure, texture, and mechanical properties analysis of novel AA7178/SiC nanocomposites. Ceram Int 2023;49:20637–50. https://doi.org/10.1016/j.ceramint.2023.03.195.
[16] Uniyal P, Gaur P, Yadav J, Khan T, Ahmed OS. A review on the effect of metal oxide nanoparticles on tribological properties of biolubricants. ACS Omega 2024;9:12436–56. https://doi.org/10.1021/acsomega.3c08279.
[17] Pawar RV, Hulwan DB, Mandale MB. Recent advancements in synthesis, rheological characterization, and tribological performance of vegetable oil-based lubricants enhanced with nanoparticles for sustainable lubrication. J Clean Prod 2022;378:134454. https://doi.org/10.1016/j.jclepro.2022.134454.
[18] Abd Elhaseeb DM, Ali MKA, Ezzat MF, Mourad M. A review of the tribological properties of nanoparticles dispersed in bio-lubricants. Proc Inst Mech Eng, Part J: J Eng Tribology 2022;237:27–52. https://doi.org/10.1177/13506501221108125.
[19] Şirin Ş, Akıncıoğlu S, Gupta MK, Kıvak T, Khanna N. A tribological performance of vegetable-based oil combined with GNPs and hBN nanoparticles on the friction-wear tests of titanium grade 2. Tribology Int 2023;181:108314. https://doi.org/10.1016/j.triboint.2023.108314.
[20] Cortes V, Sanchez K, Gonzalez R, Alcoutlabi M, Ortega JA. The Performance of SiO2 and TiO2 nanoparticles as lubricant additives in sunflower oil. Lubricants 2020;8. https://doi.org/10.3390/lubricants8010010.
[21] Yu R, Liu J, Zhou Y. Experimental study on tribological property of MoS2 nanoparticle in castor oil. J Tribology 2019;141. https://doi.org/10.1115/1.4044294.
[22] Kumar R, Gautam RK. Tribological investigation of sunflower and soybean oil with metal oxide nanoadditives. Biomass– Convers Biorefinery 2024;14:2389–401. https://doi.org/10.1007/s13399-022-02411-6.
[23] Kulkarni T, Toksha B, Chatterjee A, Naik J, Autee A. Anti-wear (AW) and extreme-pressure (EP) behavior of jojoba oil dispersed with green additive CaCO3 nanoparticles. J Eng Appl Sci 2023;70:29. https://doi.org/10.1186/s44147-023-00202-y.
[24] Gupta RN. H. A.P, Tribological study of castor oil with surface-modified CuO nanoparticles in boundary lubrication. Ind Lubr Tribology 2018;70:700–10. https://doi.org/10.1108/ILT-02-2017-0030.
[25] Kashyap A, Harsha AP. Tribological studies on chemically modified rapeseed oil with CuO and CeO2 nanoparticles. Proc Inst Mech Eng Part J J Eng Tribology 2016;230:1562–71. https://doi.org/10.1177/1350650116641328.
[26] Mahara M, Singh Y. Tribological analysis of the neem oil during the addition of SiO2 nanoparticles at different loads. Mater Today: Proc 2020;28:1412–5. https://doi.org/10.1016/j.matpr.2020.04.813.

[27] Rajaganapathy C, Vasudevan D, Murugapoopathi S. Tribological and rheological properties of palm and brassica oil with inclusion of CuO and TiO2 additives. Mater Today: Proc 2021;37:207–13. https://doi.org/10.1016/j.matpr.2020.05.032.

[28] Kerni L, Raina A, Haq MIU. Friction and wear performance of olive oil containing nanoparticles in boundary and mixed lubrication regimes. Wear 2019;426-427:819–27. https://doi.org/10.1016/j.wear.2019.01.022.

[29] Mousavi SB, Pourpasha H, Heris SZ. High-temperature lubricity and physicochemical behaviors of synthesized Cu/TiO2/MnO2-doped GO nanocomposite in high-viscosity index synthetic biodegradable PAO oil. Int Commun Heat Mass Transf 2024;156:107642. https://doi.org/10.1016/j.icheatmasstransfer.2024.107642.

[30] Mariño F, Liñeira del Río JM, R E, López J, Fernández. Chemically modified nanomaterials as lubricant additive: time stability, friction, and wear. J Mol Liq 2023;382:121913. https://doi.org/10.1016/j.molliq.2023.121913.

[31] Chen Y, Renner P, Liang H. Dispersion of nanoparticles in lubricating oil: a critical review. Lubricants 2019;7. https://doi.org/10.3390/lubricants7010007.

[32] Ivanov M, Shenderova O. Nanodiamond-based nanolubricants for motor oils. Curr Opin Solid State Mater Sci 2017;21:17–24. https://doi.org/10.1016/j.cossms.2016.07.003.

[33] López-López M, Kuzhir P, Bossis G, Mingalyov P. Preparation of well-dispersed magnetorheological fluids and effect of dispersion on their magnetorheological properties. Rheol Acta 2008;47:787–96. https://doi.org/10.1007/s00397-008-0271-6.

[34] Commission Decision (EU) 2018/1702 of 8 November 2018 establishing the EU Ecolabel criteria for lubricants (notified under document C(2018) 7125), (Accessed 01 July 2024).

[35] Sunqing Q, Junxiu D, Guoxu C. Wear and friction behaviour of CaCO3 nanoparticles used as additives in lubricating oils 2000;12:205–12. https://doi.org/10.1002/ls.3010120207.

[36] Zhang M, Wang X, Fu X, Xia Y. Performance and anti-wear mechanism of CaCO3 nanoparticles as a green additive in poly-alpha-olefin. Tribology Int 2009;42:1029–39. https://doi.org/10.1016/j.triboint.2009.02.012.

[37] Mirghani M, Man Y. Determination of hexane residues in vegetable oils with FTIR spectroscopy. J Oil Fat Ind 2003;80:619–23. https://doi.org/10.1007/s11746-003-0748-3.

[38] P.L. Boey, M.I. Saleh, N. Sapawe, S. Ganesan, G.P. Maniam, D.M. Ali, A. Pyrolysis, Pyrolysis of residual palm oil in spent bleaching clay by modified tubular furnace and analysis of the products by GC-MS, 91 (2011) 199–204. ⟨https://doi.org/10.1016/j.jaap.2011.02.010⟩.

[39] Lumakso F, Rohman A, M H, Riyanto S, Yusof F. Detection and quantification of soybean and corn oils as adulterants in avocado oil using fourier transform mid infrared (FT-MIR) spectroscopy aided with multivariate calibration. J Teknol 2015;77. https://doi.org/10.11113/jt.v77.3640.

[40] Jiménez-Sanchidrián C, Ruiz JR. Use of Raman spectroscopy for analyzing edible vegetable oils. Appl Spectrosc Rev 2016;51:417–30. https://doi.org/10.1080/05704928.2016.1141292.

[41] Yang D, Ying Y. Applications of Raman spectroscopy in agricultural products and food analysis: a review. Appl Spectrosc Rev 2011;46:539–60. https://doi.org/10.1080/05704928.2011.593216.

[42] Hussein AI, Ab-Ghani Z, Che Mat AN, Ab Ghani NA, Husein A, Ab. Rahman I. Synthesis and characterization of spherical calcium carbonate nanoparticles derived from cockle shells. Appl Sci 2020;10:7170. https://doi.org/10.3390/app10207170.

[43] Liñeira del Río JM, Alba A, Guimarey MJG, Prado JI, Amigo A, Fernández J. Surface tension, wettability and tribological properties of a low viscosity oil using CaCO3 and CeF3 nanoparticles as additives. J Mol Liq 2023;391:123188. https://doi.org/10.1016/j.molliq.2023.123188.

[44] Sherazi STH, Talpur MY, Mahesar SA, Kandhro AA, Arain S. Main fatty acid classes in vegetable oils by SB-ATR-Fourier transform infrared (FTIR) spectroscopy. Talanta 2009;80:600–6. https://doi.org/10.1016/j.talanta.2009.07.030.

[45] Deepika SK, Hait Y, Chen. Optimization of milling parameters on the synthesis of stearic acid coated CaCO3 nanoparticles. J Coat Technol Res 2014;11:273–82. https://doi.org/10.1007/s11998-013-9547-6.

[46] W.J.B. Dufresne, C.J. Rufledt, C.P. Marshall, Raman spectroscopy of the eight natural carbonate minerals of calcite structure, 49 (2018) 1999–2007. ⟨https://doi.org/10.1002/jrs.5481⟩.

[47] Azimi B, Tahmasebpoor M, Sanchez-Jimenez PE, Perejon A, Valverde JM. Multicycle CO_2 capture activity and fluidizability of Al-based synthesized CaO sorbents. Chem Eng J 2019;358:679–90. https://doi.org/10.1016/j.cej.2018.10.061.

[48] Kati, M., Behaviour of Radio-Thermoluminescence (X-Ray Irradiated), Thermal and Structural Characterization of Limestone, Celal Bayar Üniversitesi Fen Bilimleri Dergisi 18 (2022) 435–441.

[49] Liñeira del Río JM, López ER, Fernández J, García F. Tribological properties of dispersions based on reduced graphene oxide sheets and trimethylolpropane trioleate or PAO 40 oils. J Mol Liq 2019;274:568–76. https://doi.org/10.1016/j.molliq.2018.10.107.

[50] Liñeira del Río JM, Alonso Pérez G, Martínez A, Peña D, Fernández J. Tribological improvement of potential lubricants for electric vehicles using double functionalized graphene oxide as additives. Tribology Int 2024;193:109402. https://doi.org/10.1016/j.triboint.2024.109402.

[51] Liñeira del Río JM, López ER, González Gómez M, Yáñez Vilar S, Piñeiro Y, Rivas J, et al. Tribological behavior of nanolubricants based on coated magnetic nanoparticles and trimethylolpropane trioleate base oil. Nanomaterials 2020;10. https://doi.org/10.3390/nano10040683.

[52] Nasser KI, Liñeira del Río JM, López ER, Fernández J. Synergistic effects of hexagonal boron nitride nanoparticles and phosphonium ionic liquids as hybrid lubricant additives. J Mol Liq 2020;311:113343. https://doi.org/10.1016/j.molliq.2020.113343.

[53] Liñeira del Río JM, Mariño F, López ER, Gonçalves DEP, Seabra JHO, Fernández J. Tribological enhancement of potential electric vehicle lubricants using coated TiO2 nanoparticles as additives. J Mol Liq 2023;371:121097. https://doi.org/10.1016/j.molliq.2022.121097.

[54] Hamrock B, Dowson D. Minimum film thickness in elliptical contacts for different regimes of fluid-film lubrication. Proc Soc Photo-Opt Instrum Eng 1978.

[55] Guimarey MJG, Gonçalves DEP, Liñeira del Río JM, Comuñas MJP, Fernández J, Seabra JHO. Lubricant properties of trimethylolpropane trioleate biodegradable oil: High pressure density and viscosity, film thickness, Stribeck curves and influence of nanoadditives. J Mol Liq 2021;335:116410. https://doi.org/10.1016/j.molliq.2021.116410.

[56] Di Battista D, Cipollone R. Experimental and numerical assessment of methods to reduce warm up time of engine lubricant oil. Appl Energy 2016;162:570–80. https://doi.org/10.1016/j.apenergy.2015.10.127.

[57] Cecilia JA, Ballesteros Plata D, Alves Saboya RM, Tavares de Luna FM, Cavalcante CL, Rodríguez-Castellón E. An overview of the biolubricant production process: challenges and future perspectives. Processes 2020;8. https://doi.org/10.3390/pr8030257.

[58] Syahir AZ, Zulkifli NWM, Masjuki HH, Kalam MA, Alabdulkarem A, Gulzar M, et al. A review on bio-based lubricants and their applications. J Clean Prod 2017;168:997–1016. https://doi.org/10.1016/j.jclepro.2017.09.106.

[59] Mata TM, Martins AA, Caetano NS. Microalgae for biodiesel production and other applications: a review. Renew Sustain Energy Rev 2010;14:217–32. https://doi.org/10.1016/j.rser.2009.07.020.

[60] Kimura, Y., Tanaka, M., PotIo, Y.J., Enomoto, M.E., Part J: Journal of Engineering Tribology, Tribology Research in Japan—A State-of-the-Art Report, 210 (1996) 159 - 172.